# Another possibility to focus moving targets by normalized relative speed in UWB SAR

Vu, Viet T., Sjögren, Thomas K. and Pettersson Mats I.

Blekinge Institute of Technology, 37179 Karlskrona, Sweden

## ABSTRACT

The paper presents another possibility to focus moving targets using normalized relative speed (NRS). Similar to the currently used focusing approach, the focusing approach proposed in this paper aims at the ultrawideband and ultrawidebeam synthetic aperture radar systems (UWB SAR) like CARABAS-II. The proposal is shown to overcome the shortcomings of the original focusing approach and can be extended to more complicated cases, for example bistatic SAR.

**Keywords:** UWB SAR, GMTI. focusing, moving target, NRS, CARABAS-II, bistatic

## 1. INTRODUCTION

Synthetic Aperture Radar (SAR) has an important role in geoscience and remote sensing applications. The ability to effectively operate in severe weather conditions is evaluated as the main advantage of SAR in comparison to other sensor systems. One of the most crucial applications of SAR is ground moving target indication (GMTI) as such application is of interest to both military and civilian end users.

The development of the GMTI methods has received a great concern of researchers. Among the available GMTI methods, the moving target detection by focusing technique[1] is considered as a promising detection technique aiming at the ultrawideband ultrawidebeam synthetic aperture radar (UWB SAR) systems such as CARABAS-II,[2] LORA[3] and P-3.[4] The detection technique facilitates slow moving target detection, which is challenging for the detection techniques based on Doppler effects, and also multiple moving target detection. It supports both single- and multi-channel SAR data and available for being integrated into both time- and frequency-domain algorithms. The technique has been experimented with different sets of data collected by CARABAS-II in different filed campaigns.[1] The improvement in Signal-to-Clutter-Noise Ratio (SCNR) measured in these experiments on single-channel SAR data is up to approximately 20 dB and the improvement is supposed to be preserved at least for the case of multi-channel SAR data. Such improvement allows detection of moving targets which may be obscured by a considerable number of surrounded stationary targets. As presented in,[1] the moving target detection by focusing technique enables initial motion parameter estimation of the detected targets like NRS. However, an extension of the technique to more complicated cases like bistatic SAR may not be possible.

The limitations of the moving target detection by focusing technique in target motion estimations originate from the assumptions in the derivation of the focusing approach. Hence, in the derivation,[1] the flight track of a platform is assumed to be parallel to the $\xi-$axis of the Cartesian coordinate system $(\xi, \eta, \zeta)$. Also, the derivation is strongly related to the minimum range, the space and time of a moving target associated with the minimum range. Applying the focusing approach allows us to focus the moving target and displace it to the coordinate where the minimum range is achieved. However, such assumptions may not be fulfilled for more complicated cases. For example, in general bistatic SAR, the flight tracks of the transmitting and receiving platforms are not parallel. The minimum ranges may not be simultaneously obtained for both the transmitting and receiving platforms.

The objective of this paper is to point out the limitation of the currently used focusing approach and to propose a new focusing approach which allows extending the technique to more complicated cases like bistatic

Further author information: (Send correspondence to Viet T. Vu)
Viet Thuy Vu: E-mail: viet.thuy.vu@bth.se, Telephone: +46 708 61 03 95

Airborne Intelligence, Surveillance, Reconnaissance (ISR) Systems and Applications X, edited by D. J. Henry, et al.,
Proc. of SPIE Vol. 8713, 87130H · © 2013 SPIE · CCC code: 0277-786X/13/$18 · doi: 10.1117/12.2015247

SAR possible. The proposal is then validated and examined with both the simulated data and the real data. CARABAS-II is selected as a reference system in this research work.

The paper is organized as follows. Section 2 reviews the current focusing approach using NRS and its limitation. The section also proposes a new focusing approach which can be applied to more complicated cases like bistatic SAR. The new equations for NRS, focusing, coordinates where a moving target is focused, target speed and direction of movement are derived in this section. In section 3, the simulations results are provided to verify the derived equations in the previous section. Section 4 investigates the possibility to extend the focusing approach to bistatic SAR. The conclusions are given in section 5.

## 2. FOCUSING MOVING TARGETS IN UWB SAR

The section reviews the currently used focusing approach as a basis of the moving target detection by focusing technique.[1] The limitations of the approach in target motion estimations are also pointed out. A new focusing approach is then proposed which overcomes those limitations.

### 2.1 Current Focusing Approach

Let's consider a monostatic SAR system in a Cartesian system $(\xi, \eta, \zeta)$. The movement of the platform is assumed to be with constant speeds, i.e. no acceleration, and linear. This monostatic SAR system is assumed to illuminate a ground scene where there is a moving target. The movement of the target on the ground is also assumed to be with constant speeds and linear. According to,[1] the movement of the target is represented by

$$\begin{aligned} \xi_{tg}(t) &= v_{tg,\xi}(t - t_0) + \xi_{tg,0} \\ \eta_{tg}(t) &= v_{tg,\eta}(t - t_0) + \eta_{tg,0} \\ \zeta_{tg}(t) &= 0 \end{aligned} \tag{1}$$

where $v_\xi$ and $v_\eta$ are the speed components of the moving target and therefore $v_{tg,\xi}^2 + v_{tg,\eta}^2 = v_{tg}$. The time $t_0$ is the time at the minimum range $r_0$. The ground coordinates of the target at $r_0$ are $\xi_{tg,0}$ and $\eta_{tg,0}$. The presentation (1) allows us to simplify the expression of the movement of the platform without losing generality as

$$\begin{aligned} \xi_{pl}(t) &= v_{pl}t \\ \eta_{pl}(t) &= 0 \\ \zeta_{pl}(t) &= \zeta_{pl,0} \end{aligned} \tag{2}$$

where $v_{pl}$ is the speed of the platform and $\zeta_{pl,0}$ is the flight altitude. The expressions (1) and (2) allow us to estimate NRS to focus the moving target as well as the coordinates $(x_0, r_0)$ where the target is focused in a SAR image as

$$\gamma = \sqrt{\frac{(v_{pl} - v_{tg,\xi})^2 + v_{tg,\eta}^2}{v_{pl}^2}} \tag{3}$$

$$x_0 = \xi_{tg,0} - \frac{v_{tg,\eta}}{v_{pl} - v_{tg,\xi}}\eta_{tg,0} \tag{4}$$

and

$$r_0 = \sqrt{\eta_{tg,0}^2\left[1 + \left(\frac{v_{tg,\eta}}{v_{pl} - v_{tg,\xi}}\right)^2\right] + \zeta_{pl,0}^2} \tag{5}$$

Applying this focusing approach to more complicated cases like bistatic SAR may not be possible. Hence, for the general bistatic geometry, we cannot have the assumption (2) for both the transmitting and receiving platforms. There may not exists the coordinates $(\xi_{tg,0}, \eta_{tg,0})$ which result in the minimum ranges to the platforms, simultaneously.

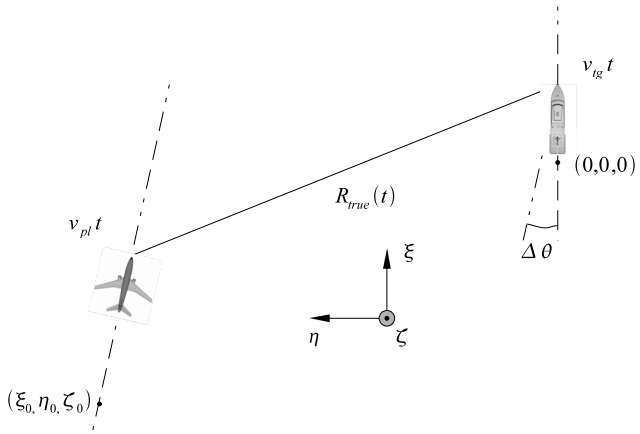


Figure 1. Monostatic SAR system geometry.

### 2.2 Proposed Focusing Approach

Let's us consider the same SAR system. We attach a Cartesian system $(\xi, \eta, \zeta)$ to this SAR system as illustrated in Fig. 1. All movements are assumed to be with constant speeds and linear. Instead of using (2) to express the movement of the platform, we use a more general form as follows

$$\begin{aligned} \xi_{pl}(t) &= v_{pl,\xi}t + \xi_0 \\ \eta_{pl}(t) &= v_{pl,\eta}t + \eta_0 \\ \zeta_{pl}(t) &= \zeta_0 \end{aligned} \tag{6}$$

where $v_{pl,\xi} = v_{pl}\cos\Delta\theta$ and $v_{pl,\eta} = v_{pl}\sin\Delta\theta$ are the platform speed components and therefore $\sqrt{v_{pl,\xi}^2 + v_{pl,\eta}^2} = v_{pl}$. The initial coordinates of the platform in a Cartesian coordinate system are given by $(\xi_0, \eta_0, \zeta_0)$. Without losing generality, the movement of the target can represented using the same Cartesian coordinate system as

$$\begin{aligned} \xi_{tg}(t) &= v_{tg}t \\ \eta_{tg}(t) &= 0 \\ \zeta_{tg}(t) &= 0 \end{aligned} \tag{7}$$

The true radar range − the half-way traveling distance of a radar pulse originated from the transmitter impinging on a target on the SAR scene and scattered back to the receiver − is calculated by

$$R_{true}(t) = \sqrt{\left(v_{pl,\xi}t + \xi_0 - v_{tg}t\right)^2 + \left(v_{pl,\eta}t + \eta_0\right)^2 + \zeta_0^2} \tag{8}$$

If the true range history of the moving target (7) is used to reconstruct a SAR image, the moving target is defocused in the SAR image in the form of either hyperbolic or elliptic curve. According to the concept of the relative speed between two objects in motion, one moving object is seen to be stationary for the other which moves with the relative speed between them. Thus, the moving target can be seen to be stationary for the platform if the platform is assumed to move with the relative speed. This principle has been used to focus the moving target in the SAR image. According to,[1] in the SAR image formation process, if the moving target is displaced and focused at the coordinates $(x_0, y_0)$ in a image coordinate system $(x, y, z)$, there will be an NRS which satisfies the following circumstance during the integration time

$$\begin{aligned} R_{est}(t) &= R_{true}(t) \\ &= \sqrt{\left(\gamma v_{pl,\xi}t + \xi_0 - x_0\right)^2 + \left(\gamma v_{pl,\eta}t + \eta_0 - y_0\right)^2 + z_0^2} \end{aligned} \tag{9}$$

where $\zeta_0 \equiv z_0$. Equation (9) is the focusing equation in monostatic SAR. Taking (8) into account, the circumstance (9) has the form $\sqrt{a} = \sqrt{b}$. To solve such equation in order to find $\gamma$, we first take the square both sides of the equation. This result in a new equation

$$\left(v_{pl,\xi}t + \xi_0 - v_{tg}t\right)^2 + \left(v_{pl,\eta}t + \eta_0\right)^2 + \zeta_0^2 = \left(\gamma v_{pl}t + \xi_0 - x_0\right)^2 + \left(\gamma v_{pl,\eta}t + \eta_0 - y_0\right)^2 + z_0^2 \tag{10}$$

Equation (10) is a second order equation and has the form $at^2 + bt + c = 0$. However, to be assure that the condition (10) satisfies at any time $t$ during the integration time, the following set of equations, which corresponds to the terms $t^0$, $t^1$ and $t^2$, must be fulfilled

$$\begin{cases} \xi_0^2 + \eta_0^2 - \left(\xi_0 - x_0\right)^2 - \left(\eta_0 - y_0\right)^2 = 0 \\ \left(v_{pl,\xi} - v_{tg}\right)\xi_0 + v_{pl,\eta}\eta_0 \\ \quad -\gamma\left[v_{pl,\xi}\left(\xi_0 - x_0\right) + v_{pl,\eta}\left(\eta_0 - y_0\right)\right] = 0 \\ \left(v_{pl,\xi} - v_{tg}\right)^2 + v_{pl,\eta}^2 - \gamma^2\left(v_{pl,\xi}^2 + v_{pl,\eta}^2\right) = 0 \end{cases} \tag{11}$$

The last equation in (11) results in NRS

$$\begin{aligned} \gamma &= \frac{\sqrt{\left(v_{pl,\xi} - v_{tg}\right)^2 + v_{pl,\eta}^2}}{v_{pl}} \\ &= \frac{\sqrt{v_{pl}^2 - 2v_{tg}v_{pl}\cos\Delta\theta + v_{tg}^2}}{v_{pl}} \end{aligned} \tag{12}$$

and the first two equations in (11) give the coordinates where the target is focused $(x_0, y_0)$

$$x_0 = \frac{1}{\gamma}\left[\xi_0\left(\gamma - 1\right) + \frac{v_{tg}\left(v_{pl,\xi}\xi_0 - v_{pl,\eta}\eta_0\right)}{v_{pl}^2}\right] \tag{13}$$

$$y_0 = \frac{1}{\gamma}\left[\eta_0\left(\gamma - 1\right) + \frac{v_{tg}\left(v_{pl,\xi}\eta_0 + v_{pl,\eta}\xi_0\right)}{v_{pl}^2}\right] \tag{14}$$

For a single moving target illuminated by a monostatic SAR system, $\gamma$ and $(x_0, y_0)$ are unique. With the known motion parameters of the platform $(\xi_{pl,0}, \eta_{pl,0})$ and $v_{pl}$, and the coordinates $(x_0, y_0)$ of the focused moving target, we can easily estimate the speed of the target $v_{tg}$ and the angle formed by the platform velocity and the target velocity $\Delta\theta$ as

$$v_{tg} = v_{pl}\sqrt{\frac{\left[\gamma x_0 - \left(\gamma - 1\right)\xi_0\right]^2 + \left[\gamma y_0 - \left(\gamma - 1\right)\eta_0\right]^2}{\xi_0^2 + \eta_0^2}} \tag{15}$$

and

$$\Delta\theta = \mathrm{ArcCos}\left\{\frac{v_{pl}}{v_{tg}}\left[\gamma\left(\frac{\xi_0 x_0 + \eta_0 y_0}{\xi_0^2 + \eta_0^2}\right) - \left(\gamma - 1\right)\right]\right\} \tag{16}$$

## 3. VERIFICATION

In this section, we present some simulation results to verify (12)-(16). In the simulations, we use geometry similar to the one given in Fig. 1.

The simulated SAR system is based only on CARABAS-II's parameters in reality.[2] The main parameters of this system are summarized in Table 1. The number of aperture positions in the simulation is 3370 corresponding to a synthetic aperture of 30° with respect to the center of the simulated ground scene. The flight track forms with the $\xi-$ axis an angle of 25°. The ground scene includes one point-like scatterer located constantly in about the middle of the scene (so-called target 0) and two random moving point-like scatterers (so-called target 1 and

Table 1. Parameters of the simulated platforms.

| Parameter | CARABAS-II | LORA |
|---|---|---|
| Operating frequency range | 22 MHz−82 MHz | |
| Platform speed | 126 m/s | 130 m/s |
| Aperture step | 0.9375 m | |
| Number of aperture positions | 3370 | |
| Flight altitude | 4944 m | 2894 m |
| PRF | 137 Hz | |
| Initial coordinates | $(-1578, -3204)$ | $(-578, -4204)$ |
| Direction of movement (with respect to $\xi-$ axis) | $25^o$ | $35^o$ |

Table 2. Parameters of simulated targets in ground scene.

| Parameter | Target 0 | Target 1 | Target 2 |
|---|---|---|---|
| Scatterer's feature | Point-like | Point-like | Point-like |
| Target speed | 0 m/s | 5 m/s | 10 m/s |
| Initial coordinates | $(64, -64)$ | $(0, 0)$ | $(-256, 128)$ |
| Direction of movement (with respect to $\xi-$ axis) | | $0^o$ | $-10^o$ |
| Angle formed by flight track & target trajectory | | $25^o$ | $35^o$ |
| NRS | | 0.9642 | 0.9361 |
| Refocusing coordinates | | $\approx (55, -28)$ | $\approx (-96, 60)$ |

target 2). The parameters of the simulated target in the ground scene are summarized in the higher part of Table 2.

Fig. 2 shows the SAR image of the simulated ground scene with the Global Backprojection (GBP) algorithm[5] using the range time-dependent equation (12) or in other words using (13) where $\gamma = 1.0000$. The image sample is selected by 1 m×1 m. The SAR image includes 512×512 samples and its actual size is 512 m×512 m. As shown in Fig. 2, the stationary point-like scatterer is well focused and appears in the upper right of the SAR image as a point target while the moving point-like scatterers are defocused and appears as curves in the middle and the lower part of the SAR image.

To examine (12), i.e. to focus the moving targets in the ground scene using NRSs, instead of using (8) for GBP, we use the focusing equation given by (9) where the values of NRS, i.e. $\gamma_1$ and $\gamma_2$, are given by (12). From the movement of direction of the platform and the targets with respect to $\xi-$ axis given in Table 1 and the higher part of Table 2, the angle formed by the flight track and the target 1's trajectory will be calculated as $\Delta\theta_1 = 25^o$ and the angle corresponding to the target 2 will be $\Delta\theta_2 = 35^o$. This calculation is presented in the lower part of Table 2. With the known platform speed, the known target speeds, and the calculated angles formed by the flight track and the target trajectories in the simulation, (12) results in the the values $\gamma_1 = 0.9642$ and $\gamma_2 = 0.9361$.

The new SAR images with moving target 1 and 2 focusing are given in Fig. 3 and Fig. 4, respectively. As observed, the target 1 is now refocused with $\gamma_1$ and appears in about the middle of the SAR image as a point target in Fig. 3 whereas both the target 0 and target 2 are smeared as curves and displaced to the upper and the lower parts of the SAR image, respectively. The original feature of the target 2 is recovered with $\gamma_2$ in the lower left of the SAR image in Fig. 4 whereas other targets are defocused in the higher part of the SAR image. The refocusing of the moving targets to their original feature, i.e. the point targets, verifies (12). The refocusing

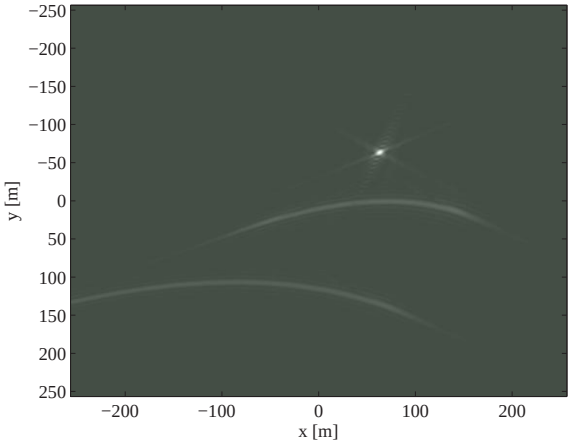


Figure 2. Simulated SAR image of the simulated ground scene. The image is reconstructed with GBP using (8) or (9) where $\gamma = 1.0000$.

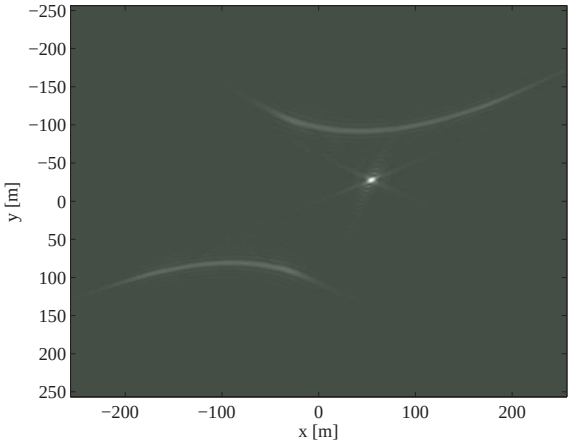


Figure 3. Simulated SAR image with moving target focusing. The image is reconstructed with GBP using (9) where $\gamma$=0.9642.

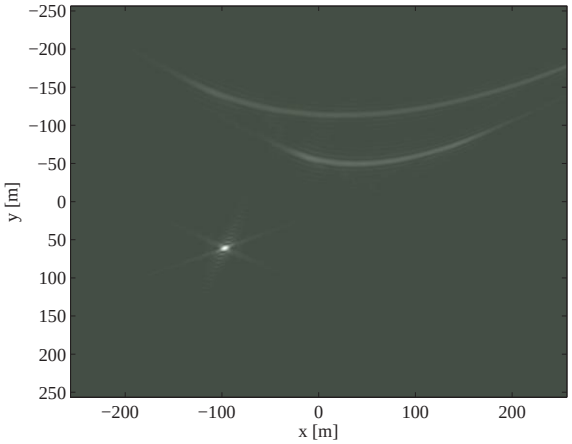


Figure 4. Simulated SAR image with moving target focusing. The image is reconstructed with GBP using (9) where $\gamma$=0.9361.

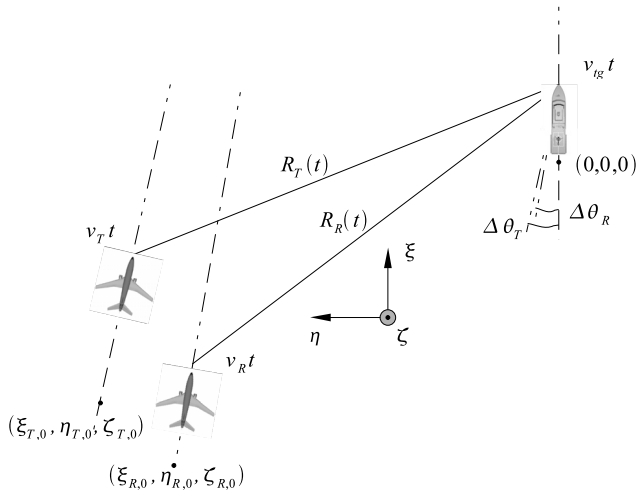


Figure 5. Bistatic SAR system geometry.

moving targets and defocusing stationary targets including clutter at the time is the basis for the moving target detection by focusing technique.

To verify (13) and (14), we first estimate the coordinates, where the moving targets are refocused, given by (13) and (14) and then compare with the true coordinates in Fig. 3 and Fig. 4. With the initial coordinates of the platform, the speed of the platform, the angle formed by the flight track and the target 1 trajectory in the simulation, and the NRS determined by (12), (13) and (14) results in the coordinates $(55.4815, -27.9299)$ where the target 1 are refocused. This result is almost identical to the true coordinates of the refocused target 1 in the SAR image in Fig. 3. For the target 2, we need to take the direction of movement and the initial coordinates of the target into account in (13) and (14). The coordinates, where the target 2 is refocused, is shown to be $(-95.5574, 59.7734)$. This calculation result is quite matched to the true coordinates of the refocused target 1 in the SAR image in Fig. 3. The differences between the results are only due to the selected image sample.

The validation of (15) and (16) can be implemented easily by a comparison between the calculations by (15) and (16) and the true values used in the simulation.

## 4. EXTENSION OF FOCUSING APPROACH TO BISTATIC

Let us consider a bistatic SAR system whose geometry is illustrated in Fig. 5. The transmitter and receiver are carried by two separated platforms. The subscript $T$ and $R$ are used here to indicate the transmitter and receiver. The expression (6) can still be used to present the movements of the platforms as

$$\begin{aligned} \xi_T(t) &= v_{T,\xi}t + \xi_{T,0} \\ \eta_T(t) &= v_{T,\eta}t + \eta_{T,0} \\ \zeta_T(t) &= \zeta_{T,0} \end{aligned} \tag{17}$$

and

$$\begin{aligned} \xi_R(t) &= v_{R,\xi}t + \xi_{R,0} \\ \eta_R(t) &= v_{R,\eta}t + \eta_{R,0} \\ \zeta_R(t) &= \zeta_{R,0} \end{aligned} \tag{18}$$

while the expression (6) is still available to present the movement of the target without losing the generality. We can easily find the focusing equation for bistatic cases as

$$\begin{aligned} \tilde{R}_{est}(t) &= \tilde{R}_{true}(t) \\ &= \left\{(\gamma_T v_{T,\xi}t + \xi_{T,0} - x_0)^2 + (\gamma_T v_{T,\eta}t + \eta_{T,0} - y_0)^2 + z_{T,0}^2\right\}^{\frac{1}{2}} \\ &+ \left\{(\gamma_R v_{R,\xi}t + \xi_{R,0} - x_0)^2 + (\gamma_R v_{R,\eta}t + \eta_{R,0} - y_0)^2 + z_{R,0}^2\right\}^{\frac{1}{2}} \end{aligned} \tag{19}$$

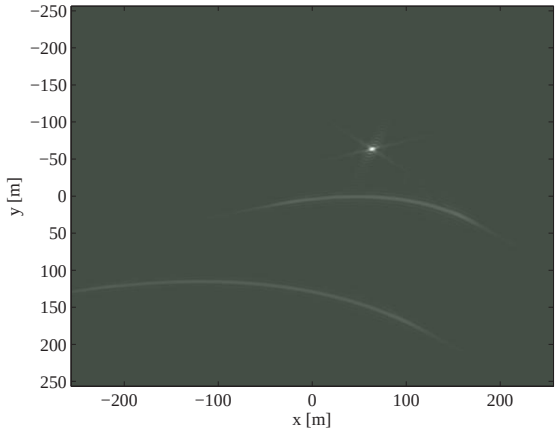


Figure 6. Simulated SAR image of the simulated ground scene. The image is reconstructed with GBP using (19) where $\gamma_T = 1.0000$ and $\gamma_R = 1.0000$.

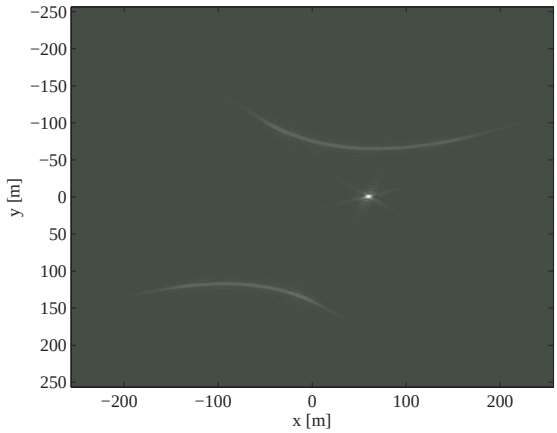


Figure 7. Simulated SAR image with moving target focusing. The image is reconstructed with GBP using (19) where $\gamma_T = 0.9642$ and $\gamma_R = 0.9688$.

where $\zeta_{T,0} \equiv z_{T,0}$ and $\zeta_{R,0} \equiv z_{R,0}$. In (19), $(\gamma_t, \gamma_r)$ are the pairs of NRS for moving target focusing. For large synthetic apertures used in UWB SAR, the pairs of NRS must satisfy the following condition

$$\gamma_T v_T - \sqrt{\left(v_{T,\xi} - v_{tg}\right)^2 + \left(v_{T,\eta}\right)^2} + \gamma_R v_R - \sqrt{\left(v_{R,\xi} - v_{tg}\right)^2 + \left(v_{R,\eta}\right)^2} = 0 \tag{20}$$

in order to focus a moving target. One example of $(\gamma_t, \gamma_r)$, which fulfills (20) and approximately focuses moving targets in most cases, is

$$\gamma_T = \frac{\sqrt{\left(v_{T,\xi} - v_{tg}\right)^2 + \left(v_{T,\eta}\right)^2}}{v_T} \tag{21}$$

and

$$\gamma_R = \frac{\sqrt{\left(v_{R,\xi} - v_{tg}\right)^2 + \left(v_{R,\eta}\right)^2}}{v_R} \tag{22}$$

There are also other pairs of $(\gamma_t, \gamma_r)$ which can be used for moving target focusing. However, the detail of this issue is skipped in this paper.

With the motion parameters of the platforms and the target 1, we can estimate NRS for the transmitting and receiving platforms as $\gamma_T = 0.9642$ and $\gamma_R = 0.9688$, respectively. The SAR image after applying the focusing

approach is given in Fig 7. The target 1, which is defocused in Fig 6, is refocused to a point target in the middle of Fig 7 whereas the the target 0 is smeared as a curve in the higher part of Fig 7. These simulation results prove the valid extension of the focusing approach to bistatic SAR.

Fig 6 shows the image of the ground scene reconstructed from the bistatic simulated SAR data using Bistatic Global Backprojection (BiGBP) algorithm.[6] The bistatic geometry in this simulation is similar to the one in Fig 5. The transmitting platform is simulated according to the CARABAS-II whereas the simulation of the receiving is based on LORA's motion parameters. The parameters of both two systems and other parameters for the simulation can be found in Table 1.

## 5. CONCLUSION

The paper presents another possibility to focus moving targets using NRS. Like the original focusing approach, the focusing approach proposed here aims at UWB SAR systems. The proposed approach is verified to work well by the simulations. It is also shown to overcome the limitations of the original focusing approach when applying to more complicated cases. Hence, the extension of the proposed approach to bistatic SAR is also sparsely investigated in this paper. A more detail investigation of this extension will be presented in another paper.

## ACKNOWLEDGMENTS

The authors would like to thank the KK-Foundation for making this research project possible, and the support from Swedish Defence Research Agency, Saab Bofors Dynamics, Saab Microwave Systems and RUAG Aerospace Sweden.

## REFERENCES

[1] Vu, V. T., Sjögren, T. K., Pettersson, M. I., Gustavsson, A., and Ulander, L. M. H., "Moving targets detection by focusing in UWB SAR - Theory and experimental results," *IEEE Trans. Geosci. Remote Sensing* **48(10)**, 3799–3815 (2010).

[2] Gustavsson, A., Ulander, L. M. H., Flood, B. H., Frölind, P.-O., Hellsten, H., Jonsson, T., Larsson, B., and Stenstrom, G., "Development and operation of an airborne VHF SAR system-lessons learned," in [*International Geoscience and Remote Sensing Symposium (IGARSS)*], *Proc. IEEE* **1**, 458–462 (1998).

[3] Ulander, L. M. H. and Hellsten, H., "Low-frequency ultrawideband array-antenna SAR for stationary and moving target imaging," in [*Radar Sensor Technology IV*], *Proc. SPIE* **3704**, 149–158 (1999).

[4] Sheen, D. R., Strawitch, C. M., and Lewis, T. B., "UHF wideband SAR design and preliminary results," in [*International Geoscience and Remote Sensing Symposium (IGARSS)*], *Proc. IEEE* **1**, 289–291 (1994).

[5] Andersson, L. E., "On the determination of a function from spherical averages," *SIAM Journal on Mathematical Analysis* **19(1)**, 214–232 (1988).

[6] Vu, V. T., Sjögren, T. K., and Pettersson, M. I., "Fast backprojection for UWB bistatic SAR," in [*Radar Conference (RADAR)*], *Proc. IEEE*, 431–434 (2011).